sciendo
Contemporary Agriculture
Serbian Journal of Agricultural Sciences
Faculty of Agriculture, University of Novi Sad, Serbia
www.contagri.info

Original scientific paper

UDC: 614.778
DOI: 10.2478/contagri-2021-0011

SAGA GIS FOR COMPUTING MULTISPECTRAL VEGETATION INDICES BY LANDSAT TM FOR MAPPING VEGETATION GREENNESS

POLINA LEMENKOVA[*]
Institute of Physics of the Earth, Russian Academy of Sciences, Laboratory of Regional Geophysics and Natural Disasters (Nr. 303), Department of Natural Disasters, Anthropogenic Hazards and Seismicity of the Earth, Bolshaya Gruzinskaya Str. 10, Bld. 1, Moscow, 123995, Russia
[*]*Corresponding author*: pauline.lemenkova@gmail.com

SUMMARY

The study presents a comparative analysis of eight Vegetation Indices (VIs) used to examine vegetation greenness over the northern coasts of Iceland. The geographical extent of the study area is set by the coordinates of the two fjords, Eyjafjörður and Skagafjörður, notable for their agricultural significance. Vegetation in Iceland is fragile due to the harsh climate, climate change, overgrazing and volcanic activity, which increase soil erosion. The study was conducted on a Landsat TM image using SAGA GIS as a technical tool for raster bands calculations. The NDVI dataset shows a range from -0.56 to 0.24, with 0 indicating 'no vegetation', and negative values – 'other surfaces' (e.g. rocks, open terrain). The DVI, compared to the NDVI, shows statistically non-normalized values ranging from -112 to 0, with extreme negative values while the coastal vegetation areas are badly distinguished from the water areas. The NRVI shows an extent from -0.24 to 0.48 with higher values for vegetation. The NRVI reduces topographic, solar and atmospheric effects and creates a normal data distribution. RVI shows a range in a dataset from 0.2 to 3.2 with vegetation in the river valleys clearly visible and depicted, while the water areas have values 0.8 to 1.0. The CTVI shows corrected TVI, in a data range -0.10 to 1.10, as the dataset of NDVI were negative. The TVI dataset ranges from 0.44 to 0.80 with the ice-covered areas and glaciers distinguishable and water values within a range from 0.60 to 0.64 and the vegetation from 0.60 to 0.44. The TTVI dataset ranges from 0.40 to 0.80 performing similarly to the TVI, but more refined with vegetation values 0.64 to 0.68. SAVI dataset ranges from -0.80 to 0.30 with minimized effects of soil on the vegetation through a constant soil adjustment factor added into the NDVI formula. The paper presents a comparison of eight VIs for Arctic vegetation monitoring. The overall behavior of SAGA GIS in calculation and mapping of the VIs is effective in terms of their use for vegetation mapping of the region.

Key words: *Iceland, vegetation indices, NDVI, SAGA GIS, cartography, mapping*

Abbreviations: VI – Vegetation Index; NDVI – Normalized Difference Vegetation Index; SAVI – Soil Adjusted Vegetation Index; RVI – Ratio Vegetation Index; NRVI – Normalized Ratio Vegetation Index; TVI – Transformed Vegetation Index; TTVI – Thiam's Transformed Vegetation Index

INTRODUCTION

Vegetation canopy defines the key landscape characteristics and its health is an indicator of the environmental processes occurring in soil-vegetation systems. Therefore, numerical assessment of green vegetation is one of the key applications of cartographic-based data assessment in remote sensing for land cover change and landscape monitoring. In this sense, understanding the distribution, greenness and quality of vegetation is a crucial step in sustainable land monitoring and mapping. This especially refers to vegetation analysis, detection of land cover

changes, defining geometric patterns of vegetation contours and natural resources monitoring (Hüttich et al., 2009; Lemenkova, 2011, 2013, 2015a; Abburu & Golla, 2015; Khan et al., 2010; Lassalle et al., 2019).
Vegetation Indices (VIs) have been introduced to analyze the distribution of vegetation and its healthiness. VIs can be used to assess green leaf area index (LAI) and canopy chlorophyll density (CCD) due to their sensitivity to canopy architecture, illumination geometry, soil background reflectance and atmospheric conditions (Broge & Leblanc, 2001). VIs differ in algorithm approach, spectral bands composition (NIR (near infra-red) and R (red) and modified combinations of NDVI), cartographic output and dimension of the results (extent of the data range). In general, VIs can be classified into two major groups according to their approach: slope-based and distance-based (Silleos et al., 2006; Jackson & Huete, 1991). The distance-based group of vegetation indices aims to cancel the effect of soil brightness where vegetation is sparse and pixels may mix green vegetation and soil background. However, such cases are mostly applied in arid and semi-arid ecosystems, which is not the case in this paper. This paper focuses on calculation and visualization of the slope-based VIs. The slope-based VIs present a combination of R and NIR bands aimed to indicate the state and abundance of green vegetation coverage and biomass. The slope-based VIs include the following indices: Normalized Difference Vegetation Index (NDVI), Soil Adjusted Vegetation Index (SAVI) developed by Qi et al. (1994), Ratio Vegetation Index (RVI), Normalized Ratio Vegetation Index (NRVI), Transformed Vegetation Index (TVI), Thiam's Transformed Vegetation Index (TTVI), and others. Among the slope-based VIs, probably the most well-known is the NDVI which is widely used in the existing literature for ecosystems monitoring (e.g. Ahmet & Akter, 2017; Lemenkova, 2014, 2015b; Raynolds et al., 2006, 2008; Pradeep Kumar et al., 2020; Nguyen et al., 2011; Zhang et al., 2020). The NDVI is a remote sensing indicator used for crop growth monitoring, farmland management and crop production prediction as well as an indicator of greenness of the biomes (Li et al., 2019).
The study area is located in northern Iceland, where the landscapes are notable for complex geological and environmental settings affected by climate change (Caseldine & Hatton, 1994; Ólafsdóttir & Guðmundsson, 2002; Tinganelli et al., 2018), overgrazing (Gísladóttir, 2001) and volcanic eruptions, creating specific types of erosion-prone soils (Arnalds et al., 2001; Arnalds, 2001, 2015). Due to limited soil development in Iceland, the vegetation is mostly sparse, dominated by heathland, wetland and other types of plants, e.g. Nootka lupin (*Lupinus nootkatensis*) (Lehnhart-Barnett & Waldron, 2020). Eddudóttir et al. (2020) recently pointed to changes in vegetation communities, soil erosion, desertification and loss of carbon stocks caused by intensive agriculture in Iceland practiced since AD 877. Geological and glaciological changes in the landscapes include modification of proglacial landsystems by repeated jökulhlaups, ice melt causing glacier margin fluctuations and retreat (Blauvelt et al., 2020). Brombacher et al. (2020) recently studied glacial ablation and river dynamics in the Þjórsá (Thjórsá) river during spring and summer by remote sensing applications using Sentinel-1 and Sentinel-2 imagery. As a result of the complex interaction of various factors, such as climate change, natural disturbances and human driven land-use changes, the landscapes in Iceland experienced catastrophic soil erosion of the heathland ecosystem, as studied by Greipsson (2012) with an example of Haukadalsheiði area.

MATERIAL AND METHODS

Software

Software used for the data processing is SAGA GIS (Böhner et al., 2008), System for Automated Geoscientific Analyses. SAGA GIS is a powerful open source GIS program for spatial data processing, mapping and raster calculations, developed originally by the University of Göttingen (Böhner et al., 2006), now maintained by a developer community. A fragment of the menu of SAGA GIS is shown in Figure 1.

Data

The data include the Landsat TM scene covering the study area. The Landsat TM imagery is often used in agricultural mapping due to their advantages in remote sensing research: the Landsat TM imagery is an open access, reliable repository with a long history, global coverage and high archiving frequency. For this study, the ortho-corrected Landsat image in WGS84 datum UTM Zone 27 was selected with the following metadata: acquisition date 2001/09/08, within the Landsat path 219, row 14. WRS type L1Gt, resampling technique cubic convolution (CC), center latitude 65°35'12.58"N, center longitude 18°30'46.09"W. The map coordinates are as follows: west 21°05'00.18"W, east 15°50'38.62"W, south 64°31'53.82"N, north 66°38'00.38"N. Image Entity ID is P219R014_7X20010908. The metadata are presented in Table 1.

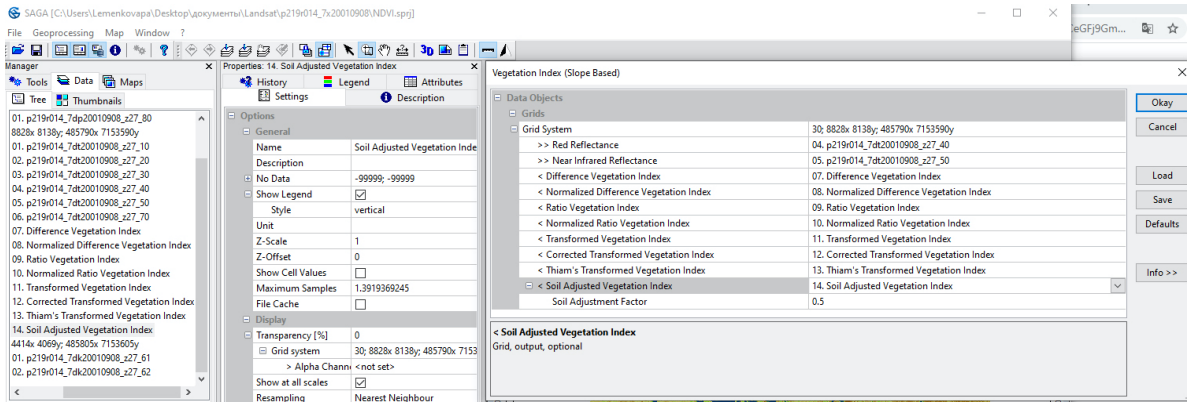

Figure 1. User interface of SAGA GIS. Source: author

Methods

Methods include technical path 'Geoprocessing> Imagery> Vegetation Indices> Vegetation Index (Slope Based)' in SAGA GIS and performed image processing. The following VIs were computed using SAGA GIS:

1. NDVI (Rouse et al., 1974) NDVI = (NIR - R) / (NIR + R), where NIR and R are the spectral reflectance in the near infrared and red wavebands.
2. DVI = NIR – R
3. RVI (Richardson & Wiegand, 1977) RVI = R / NIR
4. NRVI (Baret & Guyot, 1991) NRVI = (RVI - 1) / (RVI + 1)
5. Transformed Vegetation Index (Deering et al., 1975). TVI = [(NIR - R) / (NIR + R) + 0.5]^0.5
6. Thiam's Transformed Vegetation Index (Thiam, 1997) RVI = [abs(NDVI) + 0.5]^0.5
7. SAVI (Huete, 1988) SAVI = [(NIR - R) / (NIR + R)] * (1 + S)
8. CTVI= [SQRT(ABS (NDVI + 0.5))] (Perry & Lautenschlager, 1984)

These VIs were computed and the resulting raster maps visualized using developed algorithms of the VIs embedded in SAGA GIS for automated calculation of the satellite image spectral bands. The raster bands of the Landsat TM scene were processed and the information was extracted as calculated VIs. The R and NIR bands of the Landsat TM were inserted and VIs calculated. The VIs were displayed using adjusted color palettes to highlight the distribution of actively growing vegetation with photosynthesis processes.

Table 1. Landsat TM metadata specifications

Field	Value	Field	Value
Entity ID	P219R014_7X20010908	NW Corner Long	19°43'06.88"W
Acquisition Date	2001/09/08	NE Corner Lat	66°02'44.56"N
WRS Path	219	NE Corner Long	15°50'38.62"W
WRS Row	14	SE Corner Lat	64°31'53.82"N
WRS Type	L1Gt	SE Corner Long	17°24'06.69"W
Time Series	GLS2000	SW Corner Lat	65°04'56.62"N
Datum	WGS84	SW Corner Long	21°05'00.18"W
Zone Number	27	Center Latitude dec	65.586827
File Size	241748799	Center Longitude dec	-18.512802
Orientation	NUP	NW Corner Lat dec	66.6334386
Product Type	L1Gt	NW Corner Long dec	-19.7185772
Resampling Technique	CC	NE Corner Lat dec	66.0457106
Satellite Number	Landsat7	NE Corner Long dec	-15.8440599
Sun Azimuth	167.5457085	SE Corner Lat dec	64.5316155
Sun Elevation	29.4740846	SE Corner Long dec	-17.4018594
Center Latitude	65°35'12.58"N	SW Corner Lat dec	65.0823952
Center Longitude	18°30'46.09"W	SW Corner Long dec	-21.0833841
NW Corner Lat	66°38'00.38"N		

RESULTS AND DISCUSSION

The results of this study present a comparative analysis of eight VIs, discussed below. The NDVI (Fig. 2) produces a spectral VI that separates green vegetation from its background soil brightness. Showing the difference between NIR

and R bands, it is normalized by the sum of these bands. The advantage of the NDVI is that it minimizes the topographic effects. In the output image, the dataset ranges from -0.56 to 0.24. The dataset of the NDVI in general ranges from -1 to 1, with 0 indicating 'no vegetation', and negative values – 'other surfaces' (e.g. rocks, open terrain).

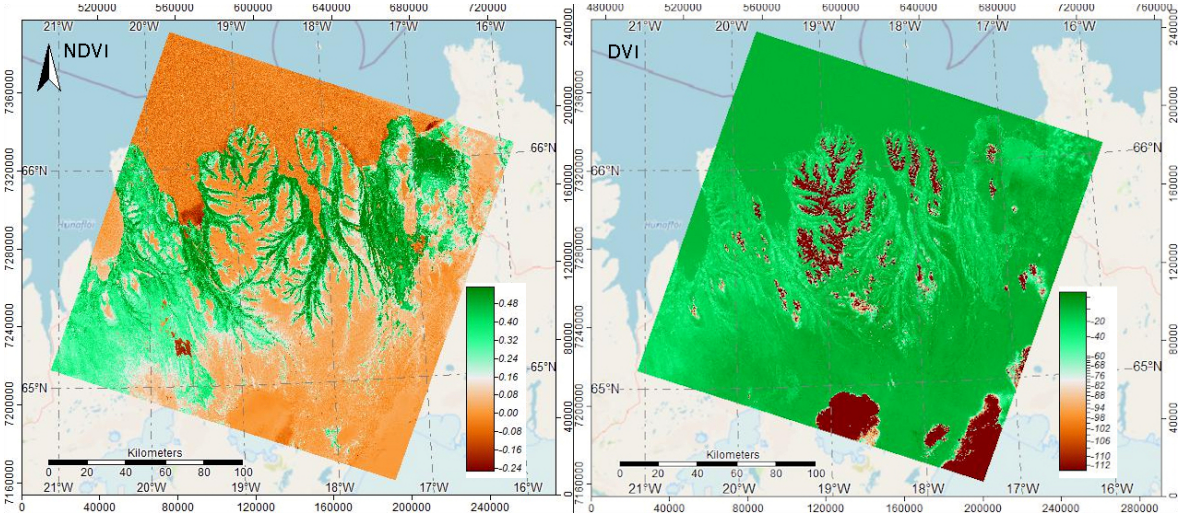

Figure 2. NDVI and DVI. Mapping: SAGA GIS. Source: author

The DVI (Fig. 2), compared to the NDVI, shows statistically non-normalized values ranging from -112 to 0, i.e. extreme negative values. The coastal vegetation areas are badly distinguished from the water areas, which proves that the NDVI has the advantages over the DVI (Fig. 2).

The NRVI (Fig. 3) shows the dataset extent from -0.24 to 0.48, with higher values for vegetation (colored as beige). The NRVI behavior is normalization and it is similar in effect to that of the NDVI, i.e. it reduces topographic, solar and atmospheric effects and creates a normal distribution.

The RVI (Fig. 3) shows a range in the dataset from 0.2 to 3.2 (roughly changing within 3). The vegetation in the river valleys is clearly visible and depicted (orange to bright red colors). In contrast, the water areas are colored purple grey with values from 0.8 to 1.0. Bright yellow colors are typical for the sandy and rocky areas and other types of the land cover surfaces.

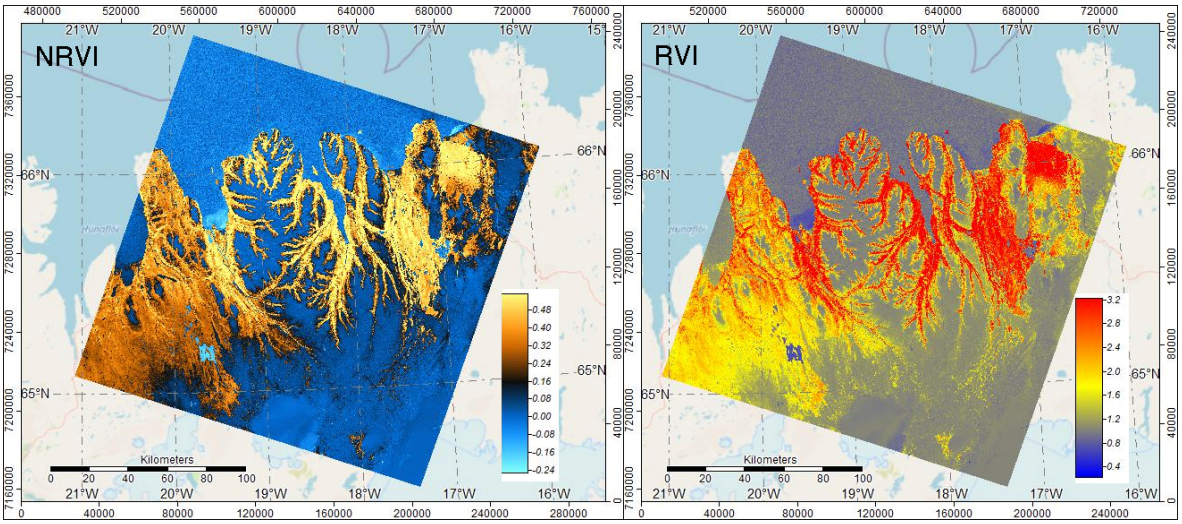

Figure 3. NRVI and RVI. Mapping: SAGA GIS. Source: author

The CTVI (Fig. 4) shows corrected TVI, which is done by adding a constant of 0.5 to all NDVI values. However, there are still some negative values in a data range (-0.10 to 1.10) because the original data values of the NDVI in a

square root were negative. The CTVI divides the expression [NDVI + 0.5] by the expression [abs(NDVI + 0.5)] multiplying it by the square root of the absolute value. Due to the sophisticated formula of the CTVI, it adjusts the values of the NDVI approaching them to the positive values suppressing the negative NDVI values. As a result, the ice-covered and lake areas are clearly visible as bright blue spots (Fig. 4). The cartographic output image of the CTVI differs from both the initial NDVI image and the TVI. However, the CTVI has a disadvantage of an overestimated vegetation class and it is not the best index compared to others.

The SAVI (Fig. 4) dataset ranges from -0.80 to 0.30. The vegetation areas are highlighted as light green colors and the glacier and ice-colored areas as dark blue colors (Fig. 4). The water areas and fjords are colored light yellow to beige. The river network is distinguishable using river patters. The rocky areas and sandy deserts are colored beige and they clearly correlate with the terrain relief (Fig. 4). Compared to the initial NDVI, the SAVI minimizes the effects of soil on the vegetation through a constant soil adjustment factor added into the NDVI algebraic formula.

The TVI (Fig. 5) demonstrates positive values due to the algebraic expression in the formula: it changes the original NDVI by an additional constant of 0.5 to the values and a square root of the results, to avoid operating with negative values of the NDVI. As a result of such adjustments, the dataset ranges from 0.44 to 0.80 (Fig. 5). Here the ice-covered areas and glaciers are clearly depicted in the image as light grey to white areas. The water areas have values within a range 0.60-0.64. The vegetation zones are colored as rose colors with values from 0.60 to 0.44.

The TTVI (Fig. 5) is done by taking the square root of the NDVI values in the TVI. The dataset ranges from 0.40 to 0.80. In this way, its performance is similar to the TVI, but more refined. Thus, the vegetation is colored as bright orange with values 0.64 to 0.68. Values of water areas range between 0.56 and 0.60 for the lakes and rivers and 0.60 to 0.64 for the ocean. In contrast to the previous VIs, the TTVI enables distinguishing the ice and glacier areas in a more precise way with gradation of water to shallow and deeper areas, as well as ice-covered zones.

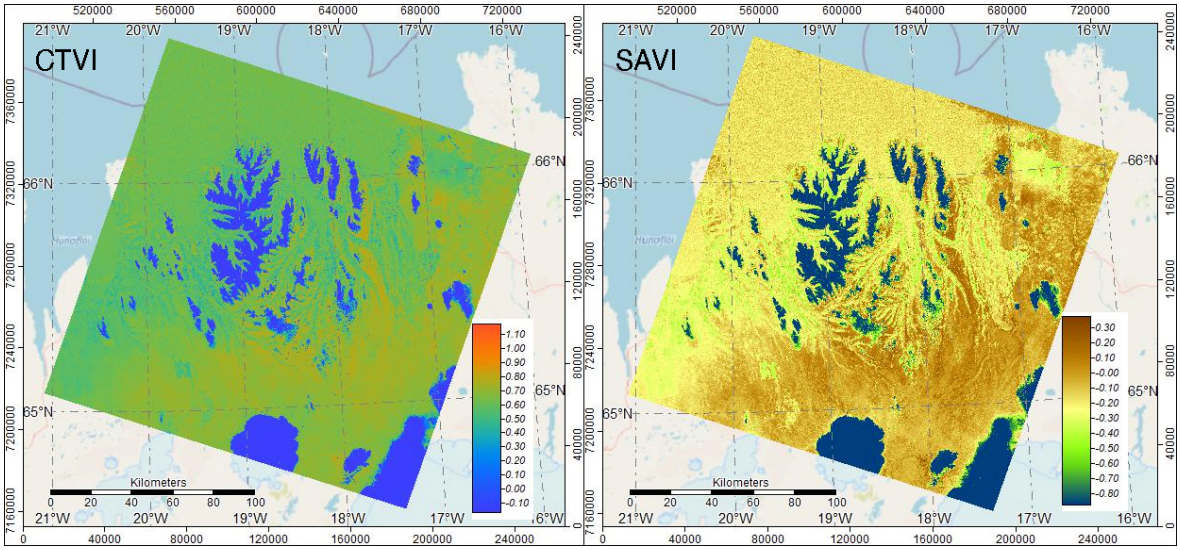

Figure 4. CTVI and SAVI. Mapping: SAGA GIS. Source: author

These results demonstrated a comparative analysis of eight VIs calculated for the coastal zone of northern Iceland with two fjords, Eyjafjörður and Skagafjörður, notable for their agricultural significance. The datasets obtained as results of the VI calculations and visualization propose other than the well-known NDVI approaches of VIs and discuss the differences in the cartographic output. Recent climate change has influenced the dynamics of the vegetation coverage in high Arctic landscapes of Iceland. This necessarily requires selective effective technical method of graphical visualization of the VIs.

Although the NDVI has become popular and widely used in previous studies, other VIs demonstrated effective visualization of vegetation and well-distinguished classification against other land cover types, such as rocks, mountains, bare soils, sandy deserts, populated areas, open water areas, river valleys, etc. SAGA GIS visualized models of various VIs showed the output representing values of vegetation coverage in various ranges, which are effective for cartographic visualization (low, moderate and high values) and selected color palettes. The use of SAGA GIS for calculating eight VIs is an excellent working solution for agricultural mapping through graphic visualization of raster VIs overlaid with the Open Street Map vector background.

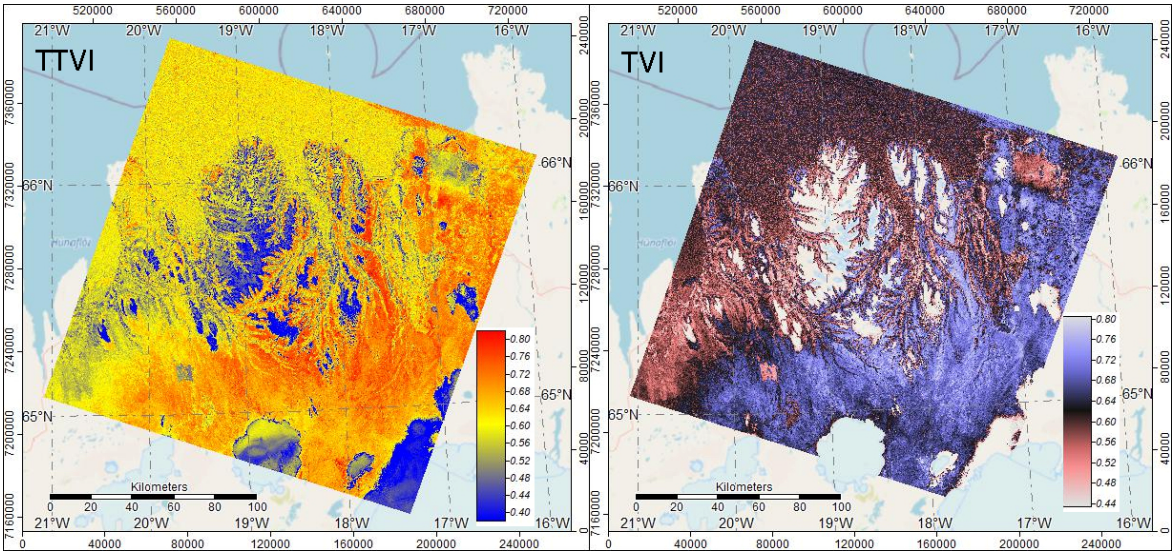

Figure 5. TTVI and TVI. Mapping: SAGA GIS. Source: author

CONCLUSION

As demonstrated in this paper, the main principle of the VIs applications refers to the properties of green vegetation which have a correlation with certain spectral bands of the satellite image. As chlorophyll strongly absorbs energy for photosynthesis in the visible regions, this property can be used to detect healthy vegetation using analysis of the satellite imagery. The absorption of chlorophyll reaches its peak in red and blue areas of electromagnetic spectrum and it is reflected in the near-infrared region. Naturally, this can be used to detect green areas of the canopy leaves. By using these variations in absorption and reflection of chlorophyll in visible, red and infrared parts of the spectrum, the quantitative indices of vegetation were developed using remotely sensed imagery such as the Landsat TM.

Besides the presented VIs used in agriculture and vegetation monitoring, it was also proposed to apply the derived indices in the financial risk with examples of the Vegetation Condition Index, Temperature Condition Index, Vegetation Health Index as independent variables (Möllmann et al., 2020). Another example of remote sensing data processing in agricultural studies was given by Ihuoma & Madramootoo (2019), who used narrow-band hyperspectral derived indices for monitoring of the water stress in tomato plants (*Solanum lycopersicum* L.). Automated data processing using the method of convolutional neural network (CNN) and color information was used by Kerkech et al. (2018) for identifying infected areas of vegetation species. Gonçalves et al. (2019) presented further steps in VIs applications by integrating NDVI with geomorphological classification and environmental GIS-analysis. There are more reports on remote sensing image analysis using automated data processing presented in literature, for example Lemenkova (2016). Besides remote sensing image analysis, other GIS approaches in environmental monitoring include landscape metrics as an indicator of ecological significance and spatial data analysis, interpretation and evaluation using methodology of ecologic carrying capacity (Klaučo et al., 2014, 2017). Using artificial neural network, statistical analysis, programming languages or automatization as more advanced methods for spatial data processing can be recommended for future studies (Foody et al., 1997; Lemenkova, 2019a, 2019b, 2019c; Klaučo et al., 2013a, 2013b; Schenke & Lemenkova, 2008). Automatization of cartographic visualization is intended for simplifying geospatial data processing (Suetova, 2005a, 2005b; Lemenkova, 2019d, 2020a, 2020b; Gauger et al., 2007). Together with the rapid development of cartographic methods (Lemenkova, 2020c, 2020d), remote sensing has experienced remarkable progress since 1980s, updating and improving the methods of data processing aimed at higher precision and speed of mapping technologies.

A feasible approach to mapping and monitoring vegetation can be achieved by calculation of combined selected raster bands in satellite imagery. However, vegetation mapping using the Landsat TM scenes may include misinterpretations, since certain pixels can be misclassified as other land cover types, especially the ones with similar spectral reflectance properties. In order to solve this problem, various algorithms of VIs have been developed to adjust and refine VI as much as possible. These VIs are presented in this paper as a comparative analysis with technical support of SAGA GIS. In general, computing vegetation indices using the Landsat TM scenes is an effective method in agricultural mapping in modern cartography used to obtain precise and accurate visualization of

the vegetation coverage (Jensen, 2005; He et al., 2016). However, due to the variety of indices, selecting the best suitable index still remains a challenge. The results of the slope-based index calculation depend on a number of factors, such as terrain complexity of the landscape and local geomorphological settings. Other important factors include the resolution and cloudiness of the raw data, the approach of the remote sensing image processing and VI calculation method. The aim of this paper was to demonstrate the variety of VIs that can be used to derive information from the Landsat TM images for the northern coasts of Iceland. The paper demonstrated eight different VIs computed and cartographically visualized using SAGA GIS for the area covering northern Iceland.

***Acknowledgements*:** I thank two anonymous reviewers and the editor for corrections and comments on the manuscript.

REFERENCES

Abburu S. & Golla S.B. (2015): Satellite Image Classification Methods and Techniques: A Review. *International Journal of Computer Applications*, 119(8): 20-25.

Ahmet K.R. & Akter S. (2017): Analysis of landcover change in southwest Bengal delta due to floods by NDVI, NDWI and K-means cluster with landsat multi-spectral surface reflectance satellite data. *Remote Sensing Applications: Society and Environment*, 8: 168-181.

Arnalds O. (2001*)*: *Soil Erosion in Iceland*. Agricultural Research Institute, Soil Conservation. Service, Reykjavík.

Arnalds O., Gisladottir F., Sigurjonsson H. (2001): Sandy deserts of Iceland: an overview. *Journal of Arid Environments*, 47: 359-371.

Arnalds O. (2015): The Soils of Iceland. Springer, Dordrecht.

Baret F. & Guyot G. (1991): Potential and limitations of vegetation indices for LAI and APAR assessment. *Remote Sensing of Environment*, 104: 88-95.

Blauvelt D.J., Russell A.J., Large A.R.G., Tweed F.S., Hiemstra J.F., Kulessa B., Evans D.J.A., Waller R.I. (2020): Controls on jökulhlaup-transported buried ice melt-out at Skeiðarársandur, Iceland: Implications for the evolution of ice-marginal environments. *Geomorphology*, 360: 107-164.

Böhner J., McCloy K.R., Strobl J. (2006): *SAGA – Analysis and Modelling Applications*. Göttinger Geographische Abhandlungen.

Böhner J., Blaschke T., Montanarella L.(2008): *SAGA – Seconds Out*. Hamburger Beiträge zur Physischen Geographie und Landschaftsökologie, 19.

Broge N.H. & Leblanc E. (2001): Comparing prediction power and stability of broadband and hyperspectral vegetation indices for estimation of green leaf area index and canopy chlorophyll density. *Remote Sensing of Environment*, 76: 156-172.

Brombacher J., Reiche J., Dijksma R., Teuling A.J. (2020): Near-daily discharge estimation in high latitudes from Sentinel-1 and 2: A case study for the Icelandic Þjórsá river. *Remote Sensing of Environment*, 241: 111684.

Caseldine C. & Hatton J. (1994): Interpretation of Holocene climatic change for the Eyjafördur area of northern Iceland from pollen-analytical data: comments and preliminary results. In: Stötter, J., Wilhelm, F. (eds). *Environmental Change in Iceland*. Münchener Geographische Abhandlungen, Reihe B, 12: 41-42.

Deering D.W., Rouse J.W., Haas R.H. & Schell J.A. (1975): Measuring "Forage Production" of Grazing Units From Landsat MSS Data. *Proceedings of the 10th International Symposium on Remote Sensing of Environment*, II: 1169-1178.

Eddudóttir S.D., Erlendsson E., Gísladóttir G. (2020): Landscape change in the Icelandic highland: A long-term record of the impacts of land use, climate and volcanism. *Quaternary Science Reviews*, 240: 106363.

Foody G.M., Lucas R.M., Curran P.J., Honzak M. (1997): Mapping tropical forest fractional cover from coarse spatial resolution remote sensing imagery. *Plant Ecology*, 131: 143-154.

Gauger S., Kuhn G., Gohl K., Feigl T., Lemenkova P., Hillenbrand C. (2007): Swath-bathymetric mapping. *Reports on Polar and Marine Research*, 557: 38-45.

Gísladóttir G. (2001): *Ecological Disturbance and Soil Erosion on Grazing Land in Southwest Iceland, Land Degradation.* Springer, 109-126.

Greipsson S. (2012): Catastrophic soil erosion in Iceland: impact of long-term climate change, compounded natural disturbances and human driven landuse changes. *Catena*, 98: 41-54.

Gonçalves R.M., Saleem A., Queiroz H.A.A., Awange J.L. (2019): A fuzzy model integrating shoreline changes, NDVI and settlement influences for coastal zone human impact classification. *Applied Geography*, 113: 102093.

He L., Zhang H., Zhang Y., Song X., Feng W., Kang G., Wang C., Guo T. (2016): Estimating canopy leaf nitrogen concentration in winter wheat based on multi-angular hyperspectral remote sensing. *European Journal of Agronomy*, 73: 170-185.

Huete A.R. (1988): A soil-adjusted vegetation index (SAVI). *Remote Sensing of Environment*, 25(3): 295-309.

Hüttich C., Gessner U., Herold M., Strohbach B.J., Schmidt M., Keil M., Dech S. (2009): On the suitability of MODIS time series metrics to map vegetation types in dry savanna ecosystems: a case study in the Kalahari of NE Namibia. *Remote Sensing*, 1(4): 620-643.

Ihuoma S.O. & Madramootoo C.A. (2019): Sensitivity of spectral vegetation indices for monitoring water stress in tomato plants. *Computers and Electronics in Agriculture*, 163: 104860.

Jackson R.D. & Huete A.R. (1991): Interpreting vegetation indices. *Preventive Veterinary Medicine*, 11: 185-200.

Jensen J.R. (2005): *Thematic map accuracy assessment. In Introductory Digital Image Processing–A Remote Sensing Perspective*, (3rd ed) Keith, C.C., Prentice Hall Series in Geographic Information Science: Saddle River, NJ, USA, 495-515.

Khan M.R., de Bie C.A.J.M., van Keulen H., Smaling E.M.A., Real R. (2010): Disaggregating and mapping crop statistics using hypertemporal remote sensing. *International Journal of Applied Earth Observation and Geoinformation*, 12: 36-46.

Kerkech M., Hafiane A., Canals R. (2018): Deep leaning approach with colorimetric spaces and vegetation indices for vine diseases detection in UAV images. *Computers and Electronics in Agriculture*, 155: 237-243.

Klaučo M., Gregorová B., Stankov U., Marković V., Lemenkova P. (2013a): Determination of ecological significance based on geostatistical assessment: a case study from the Slovak Natura 2000 protected area. *Open Geosciences*, 5(1): 28-42.

Klaučo M., Gregorová B., Stankov U., Marković V., Lemenkova P. (2013b): Interpretation of Landscape Values, Typology and Quality Using Methods of Spatial Metrics for Ecological Planning. *Environmental and Climate Technologies*, October 14, 2013. Riga, Latvia.

Klaučo M., Gregorová B., Stankov U., Marković V., Lemenkova P. (2014): Landscape metrics as indicator for ecological significance: assessment of Sitno Natura 2000 sites, Slovakia. *Ecology and Environmental Protection*, March 19-20, 2014. Minsk, Belarus, 85-90.

Klaučo M., Gregorová B., Koleda P., Stankov U., Marković V., Lemenkova P. (2017): Land planning as a support for sustainable development based on tourism: A case study of Slovak Rural Region. *Environmental Engineering and Management Journal*, 2(16): 449-458.

Lassalle G., Credoz A., Hédacq R., Bertoni G., Dubucq D., Fabre S., Elger A. (2019): Estimating persistent oil contamination in tropical region using vegetation indices and random forest regression. *Ecotoxicology and Environmental Safety*, 184: 109654.

Lehnhart-Barnett H. & Waldron S. (2020): The influence of land cover, including Nootka lupin, on organic carbon exports in east Icelandic rivers. *Catena*, 184: 104245.

Lemenkova P. (2011): *Seagrass Mapping and Monitoring Along the Coasts of Crete, Greece*. M.Sc. Thesis. University of Twente, Faculty of Earth Observation and Geoinformation (ITC), Enschede, Netherlands.

Lemenkova P. (2013): Monitoring Changes in Agricultural Landscapes of Central Europe, Hungary: Application of ILWIS GIS for Image Processing. 12th EAGE International Conference on Geoinformatics - Theoretical and Applied Aspects, Ukraine, Kiev, 13-16 May, 2013.

Lemenkova P. (2014): Detection of Vegetation Coverage in Urban Agglomeration of Brussels by NDVI Indicator Using eCognition Software and Remote Sensing Measurements. In: *GIS and Remote Sensing*. November 17-19, 2014, Tsaghkadzor, Armenia, 112-119.

Lemenkova P. (2015a): Modelling Landscape Changes and Detecting Land Cover Types by Means of the Remote Sensing Data and ILWIS GIS. *Information Technologies. Problems and Solutions*, 2: 265-271.

Lemenkova P. (2015b): Analysis of Landsat NDVI Time Series for Detecting Degradation of Vegetation. In: *Geoecology and Sustainable Use of Mineral Resources. From Science to Practice*, Belgorod, Russia, 11-13.

Lemenkova P. (2016): Using GIS for Monitoring Lacustrine Ecosystem: a Case Study of Laguna de Gallocanta, Spain. *Problems of the Environmental Landscape Planning*, 237–240.

Lemenkova P. (2019a): Statistical Analysis of the Mariana Trench Geomorphology Using R Programming Language. *Geodesy and Cartography*, 45(2): 57-84.

Lemenkova P. (2019b): GMT Based Comparative Analysis and Geomorphological Mapping of the Kermadec and Tonga Trenches, Southwest Pacific Ocean. *Geographia Technica*, 14(2): 39-48.

Lemenkova P. (2019c): AWK and GNU Octave Programming Languages Integrated with Generic Mapping Tools for Geomorphological Analysis. *GeoScience Engineering*, 65(4): 1-22.

Lemenkova P. (2019d): Geomorphological modelling and mapping of the Peru-Chile Trench by GMT. *Polish Cartographical Review*, 51(4): 181-194.

Lemenkova P. (2020a): GMT Based Comparative Geomorphological Analysis of the Vityaz and Vanuatu Trenches, Fiji Basin. *Geodetski List*, 74(1): 19-39.

Lemenkova P. (2020b): Variations in the bathymetry and bottom morphology of the Izu-Bonin Trench modelled by GMT. *Bulletin of Geography. Physical Geography Series*, 18(1): 41-60.

Lemenkova P. (2020c): NOAA Marine Geophysical Data and a GEBCO Grid for the Topographical Analysis of Japanese Archipelago by Means of GRASS GIS and GDAL Library. *Geomatics and Environmental Engineering*, 14(4): 25-45.

Lemenkova P. (2020d): Using GMT for 2D and 3D Modeling of the Ryukyu Trench Topography, Pacific Ocean. *Miscellanea Geographica*, 25(3): 1-13.

Li C., Li H., Li J., Lei Y., Li C., Manevski K., Shen Y. (2019): Using NDVI percentiles to monitor real-time crop growth. *Computers and Electronics in Agriculture*, 162: 357-363.

Möllmann J., Buchholz M., Kölle W., Musshoff O. (2020): Do remotely-sensed vegetation health indices explain credit risk in agricultural microfinance? *World Development*, 127: 104771.

Nguyen T.T.H., De Bie C.A.J.M., Ali A., Smaling E.M.A., Chu T.H. (2011): Mapping the irrigated rice cropping patterns of the Mekong delta, Vietnam, through hyper-temporal SPOT NDVI image analysis. *International Journal of Remote Sensing*, 33: 415-434.

Ólafsdóttir R. & Guðmundsson H. (2002): Holocene land degradation and climatic change in northeastern Iceland. *Holocene*, 12: 159-167.

Perry C.Jr. & Lautenschlager L.F. (1984): Functional Equivalence of Spectral Vegetation Indices, *Remote Sensing of Environment*, 14(1-3): 169-182.

Pradeep Kumar B., Raghu Babu K., Ramachandra M., Krupavathi C., Narayana Swamy B., Sreenivasulu Y., Rajasekhar M. (2020): Data on identification of desertified regions in Anantapur district, Southern India by NDVI approach using remote sensing and GIS. *Data in Brief*, 30: 105560.

Qi J., Chehbouni A., Huete A.R., Kerr Y.H., Sorooshian S. (1994): A modified soil adjusted vegetation index. *Remote Sensing of Environment*, 48: 119-126.

Raynolds M.K., Walker D.A., Maier H.A. (2006): NDVI patterns and phytomass distribution in the circumpolar Arctic. *Remote Sensing of Environment*, 102(3-4): 271-281.

Raynolds M.K., Comiso J.C., Walker D.A., Verbyla D. (2008): Relationship between satellite-derived land surface temperatures, arctic vegetation types, and NDVI. *Remote Sensing of Environment*, 112(4): 1884-1894.

Richardson A.J. & Wiegand C.L. (1977): Distinguishing Vegetation From Soil Background Information. *Photogramnetric Engineering and Remote Sensing*, 43(12): 1541-1552.

Rouse J.W, Haas R.H., Scheel J.A. & Deering D.W. (1974): Monitoring Vegetation Systems in the Great Plains with ERTS. *Proceedings, 3rd Earth Resource Technology Satellite (ERTS) Symposium*, 1: 48-62.

Schenke H.W. & Lemenkova P. (2008): Zur Frage der Meeresboden-Kartographie: Die Nutzung von AutoTrace Digitizer für die Vektorisierung der Bathymetrischen Daten in der Petschora-See. *Hydrographische Nachrichten*, 81: 16-21.

Silleos, G.N., Alexandridis, T., Gitas, I.Z., Perakis, K. (2006): Vegetation indices: Advances made in biomass estimation and vegetation monitoring in the last 30 years. *Geocarto International*, 21(4): 21-28.

Suetova I.A., Ushakova L.A., Lemenkova P. (2005a): Geoinformation mapping of the Barents and Pechora Seas. *Geography and Natural Resources*, 4: 138-142.

Suetova I.A., Ushakova L.A., Lemenkova P. (2005b): Geoecological Mapping of the Barents Sea Using GIS. In: *International Cartographic Conference (ICC)*, La Coruna, Spain.

Thiam A.K. (1997): *Geographic Information Systems and Remote Sensing. Methods for Assessing and Monitoring Land Degradation in the Sahel: The Case of Southern Mauritania*. PhD Thesis, Clark University, Worcester Massachusetts.

Tinganelli L., Erlendsson E., Eddudóttir S.D., Gísladóttir G. (2018): Impacts of climate, tephra and land use upon Holocene landscape stability in Northwest Iceland. *Geomorphology*, 322: 117-131.

Zhang H., Ma J., Chen C. & Tian X. (2020): NDVI-Net: A fusion network for generating high-resolution normalized difference vegetation index in remote sensing. *ISPRS Journal of Photogrammetry and Remote Sensing*, 168: 182-196.

Submitted: 07.09.2020.
Accepted: 20.12.2020.